Available online at www.sciencedirect.com
SCIENCE DIRECT®
Geochimica et Cosmochimica Acta 70 (2006) 827–838
Geochimica
www.elsevier.com/locate/gca

# Adsorption to goethite of extracellular polymeric substances from *Bacillus subtilis*

Anselm Omoike, Jon Chorover *

*Department of Soil, Water and Environmental Science, University of Arizona, Tucson, AZ 85721-0038, USA*

Received 17 June 2005; accepted in revised form 17 October 2005

**Abstract**

Extracellular polymeric substances (EPS) are heterogeneous biopolymers produced by Gram-negative and Gram-positive bacterial cells. Adsorption of EPS to minerals can alter the substrata physico-chemistry and influence initial bacterial adhesion processes via conditioning film formation, but the effects of solution chemistry on uptake of EPS remain poorly understood. In this study, the adsorption to goethite (α-FeOOH) of EPS isolated from the early stationary growth-phase culture of *Bacillus subtilis* was investigated as a function of pH and ionic strength (*I*) in NaCl background electrolyte using batch studies coupled with Fourier transform infrared spectroscopy and size-exclusion high-performance liquid chromatography. Proteins, particularly those of higher molar mass, and phosphorylated macromolecules were adsorbed preferentially. Increasing solution *I* (1–100 mM NaCl) or pH (3.0–9.0) resulted in a decrease in the mass of EPS adsorbed. Batch studies and diffuse reflectance infrared Fourier transform spectra are consistent with ligand exchange of EPS phosphate groups for surface hydroxyls at Fe metal centers. The data indicate that both electrostatic and chemical bonding interactions contribute to selective fractionation of the EPS solution. Proteins and phosphate groups in phosphodiester bridges of nucleic acids likely play an important role in conditioning film formation at Fe oxide surfaces.


## 1. Introduction

Continuous production of biomolecular organic matter results from the growth and metabolism of numerous Gram-negative and Gram-positive bacteria that exude extracellular polymeric substances (EPS) into their environment. These EPS are bound to the cell surface (“capsular”), released into solution (“free”) or associated with the hydrated matrix of biofilms (Wingender et al., 1999). In natural aqueous environments, pristine mineral surfaces become coated rapidly by biogenic organic films (Bos et al., 1999). The formation of these “conditioning films,” which often precedes biofilm development (Charaklis, 1990), can influence the migration and adhesion of bacterial cells in porous media by altering the surface chemistry of underlying substrate (Schneider et al., 1994). EPS are a heterogeneous mixture composed dominantly of polysaccharides and proteins, with nucleic acids and lipids as minor constituents (Wingender et al., 1999; Omoike and Chorover, 2004). The wide range in biomolecular composition, molar mass, polarity and charge, likely contributes to a comparable diversity of bonded and non-bonded interactions with natural particle surfaces. EPS contain weakly acidic functionalities that ionize in response to changes in environmental pH or ionic strength and this likely affects their environmental fate. For example, EPS isolated from the early stationary growth-phase culture of *Bacillus subtilis*—a prevalent Gram-positive soil bacteria—contain carboxyl, phosphoryl, amide, amino and hydroxyl functionalities (Omoike and Chorover, 2004). These C-, N- and P-containing moieties may interact covalently or via Coulombic or van der Waals association with hydroxylated mineral surfaces whose charge and reactivity is also dependent on solution chemistry.

Surficial conditioning of substrata by exuded EPS is well documented (e.g., Neu, 1996; Bradshaw et al., 1997; Gubner and Beech, 2000), and it has been variously suggested

* Corresponding author. Fax: +1 520 621 1647.
*E-mail address:* chorover@cals.arizona.edu (J. Chorover).

0016-7037/$ - see front matter © 2005 Elsevier Inc. All rights reserved.
doi:10.1016/j.gca.2005.10.012

that bacterial cell adhesion is mediated initially by proteinaceous (Schakenraad and Busscher, 1989; An and Friedman, 1998) or carbohydrate constituents (Davies et al., 1993; Scharfman et al., 1999). Whereas EPS molecules certainly contribute to conditioning film formation on mineral surfaces, the sorptive fractionation patterns and surface adhesion mechanism(s) remain poorly understood. We have previously observed ligand exchange of *B. subtilis* EPS phosphate groups at mineral surface hydroxyls in situ by attenuated total reflectance (ATR) Fourier transform infrared (FTIR) spectroscopy (Omoike et al., 2004). However, the extent to which this surface complexation reaction influences solid-aqueous phase partitioning of various biomacromolecules is not known. Further, the influence of important aqueous geochemical parameters on the molecular fractionation of EPS has not been studied systematically. In the present work, we investigated the adsorption of EPS isolated from the culture media of *B. subtilis* on goethite as a function of pH and ionic strength ($I$) using both macroscopic and spectroscopic techniques.

## 2. Experimental method

### 2.1. Materials

All chemicals and reagents were analytical grade and used as received. All solutions and suspensions were prepared using ultra pure (Milli-Q UV-plus) water.

### 2.2. Mineral adsorbent

Goethite was synthesized by neutralization of a 0.15 M $Fe(NO_3)_3$ solution in a high-density polyethylene bottle according to the method of Atkinson et al. (1967). The precipitate was washed several times with 1 mM HCl until the wash supernatant solution was pH 4, rinsed with ultra pure water until the conductivity of washings was the same as that of the input water, and then freeze-dried. X-ray diffraction and FTIR analysis of the freeze-dried precipitate indicated only α-FeOOH; no other solids were detected. The specific surface area of the goethite, determined by $N_2$ BET adsorption, was 44.4 $m^2\ g^{-1}$.

### 2.3. Bacterial cell cultivation, EPS isolation and purification

*Bacillus subtilis* (ATCC 7003) was cultivated aerobically in Luria broth (5.0 g $L^{-1}$ yeast extract, 10.0 g $L^{-1}$ tryptone and 5.0 g $L^{-1}$ NaCl) at 30 °C and 150 rpm (orbital shaker) to early stationary (24 h) growth phase. The cells were removed from the culture solution by centrifugation (5000 relative centrifugal force—RCF, 15 min, 4 °C) and the supernatant solution was then centrifuged at higher force (12,000 RCF, 30 min, 4 °C) to remove residual entrained cells. EPS was precipitated from the supernatant solution by adding cold reagent-grade ethanol to the supernatant solution at a volumetric ratio of 3:1, and the mixture was then stored at −20 °C for 18 h (de Brouwer et al., 2002). The precipitate was separated from the ethanol suspension by centrifugation (12,000 RCF, 30 min and 4 °C). The pellet obtained after centrifugation was dialyzed against Milli-Q water using Spectra/Por 7 regenerated cellulose (RC) membranes (1000 MWCO from Spectrum) to remove low molecular weight impurities including ethanol. After dialysis for 72 h against two changes of Milli-Q water per day, the EPS solution was freeze-dried.

### 2.4. Adsorption experiments

Adsorption envelope (variable pH) and isotherm (variable [EPS]) experiments were conducted at 296 K for 6 h equilibration time in batch mode using 50 mL Teflon centrifuge tubes as reaction vessels. EPS (0.4 g $kg^{-1}$ C) and goethite (25.0 g $kg^{-1}$ α-FeOOH) stock suspensions were prepared using $N_2$ degassed background NaCl electrolyte solutions at $I$ of 1, 10 and 100 mM. The pH was adjusted to desired values using 0.01 M HCl or 0.01 M NaOH solution. Stock suspensions were allowed to pre-equilibrate overnight prior to adsorption experiments.

#### 2.4.1. Adsorption envelopes

EPS adsorption envelope studies were conducted in 10 mM NaCl at pH values of 3.0–9.0. Stock goethite suspensions, EPS solutions and background electrolyte solutions were each prepared at initial pH values of 3.0, 4.5, 6.0 and 9.0. Stock EPS and background electrolyte solutions at the chosen pH were added to centrifuge tubes that were then capped and the contents mixed by inversion. Aliquots of the goethite stock suspensions were added to each tube to initiate the adsorption reaction at the desired initial pH. Suspension EPS and goethite concentrations in the reaction vessels were 140 mg $kg^{-1}$ C and 5 g $kg^{-1}$ α-FeOOH, respectively. All suspensions were duplicated and EPS blanks (no goethite) were included as controls for each pH. The suspensions were rotated end-over-end at 7 rpm for 6 h. (Preliminary kinetic studies indicated no significant change after 4 h.) The suspensions were then centrifuged (21,875 RCF, 30 min, 296 K), the supernatant solutions were decanted into glass vials, and solution pH was determined immediately. The amount of EPS sorbed to goethite was measured on the basis of organic C, N and P concentration depletion in the aqueous phase relative to the mineral-free blank. Aliquots of supernatant solution were employed for chromatographic (see Section 2.6) and spectroscopic (see Section 2.7) analyses. The solid phase was freeze-dried prior to spectroscopic analysis.

#### 2.4.2. Adsorption isotherm studies

Aliquots of EPS stock solution at pH 6.0 and 1, 10 or 100 mM NaCl were transferred into centrifuge tubes and mixed with background electrolyte solution (1, 10 or 100 mM NaCl; pH 6.0) to obtain a total mass of 24.0 g of solution with EPS-C concentrations ranging from 0 to 186 mg $L^{-1}$. These solutions were then mixed with aliquots of goethite suspension, pre-equilibrated at pH 6.0 at the

chosen $I$, to obtain a total suspension mass of 30.0 g and a goethite concentration of 5.0 g $L^{-1}$ in each reaction vessel. After 6 h equilibration, solutions and solids were separated by centrifugation prior to analysis, as in the adsorption edge experiments.

The batch adsorption data were fitted to the Langmuir isotherm equation

$$\Gamma_e = \frac{K\Gamma_{max}C_e}{1+KC_e}, \quad (1)$$

where $C_e$ is the aqueous phase EPS concentration (C, N or P basis) after 6 h equilibration time, $\Gamma_e$ is the adsorbed mass (C, N or P basis), $\Gamma_{max}$ is the maximum adsorbed mass and $K$ is an empirical affinity constant. Langmuir parameters are employed here solely as empirical tools to provide comparative measures of surface affinity and isotherm shape.

### 2.5. Chemical analysis

Measurements of pH were made using an Orion Ross semi-micro combination glass electrode and a Symphony bench top pH/ISE/conductivity (VWR, SR601C) meter, calibrated with standard buffer solutions. Aliquots of blank and suspension supernatant solutions were acidified with HCl to pH 2. The total organic C and N concentrations in the acidified samples were determined by high temperature combustion and infrared detection of $CO_2$ and NO using a Shimadzu TOC-V CSH TOC/TN analyzer (Columbia, MD). Calibration standards for C and N analysis were prepared from oven-dried potassium hydrogen phthalate [$(HO_2C)_2(COOK)$- $C_6H_4$] and potassium nitrate ($KNO_3$), respectively. Soluble P and Fe were measured by inductively coupled plasma mass spectrometer (ICP-MS, Perkin-Elmer DRC-2, SCIEX Instruments, Concord, Ontario, Canada). The linear calibration range for $^{31}P$ and $^{54}Fe$ was 0.1–1000 and 0.1–500 μg $L^{-1}$, respectively. Detection limits were 0.112 μg $L^{-1}$ for P and 0.879 μg $L^{-1}$ for Fe.

### 2.6. Size-exclusion high-performance liquid chromatography

Size-exclusion high-performance liquid chromatography (SE-HPLC) analysis of EPS was conducted on blank and suspension supernatant solutions using a Waters HPLC unit equipped with a 600 pump, a 717 plus auto sampler and 996 photodiode array (PDA) and 410 differential refractometer (refractive index, RI) detectors in series (Omoike and Chorover, 2004). Whereas PDA detects elution of UV-absorbing molecules (proteins and nucleic acids), the RI detector gives information on all macromolecular constituents that alter the refractive index of the mobile phase (inclusive of proteins, nucleic acids and polysaccharides). Thus, comparison of RI and PDA chromatograms facilitates peak assignment to dominantly protein versus polysaccharide groups. Separations were carried out in two stainless-steel (8 × 300 mm) size exclusion chromatography (SEC) columns (HEMA Bio 100 and 1000 Å, PSS Polymer Standards-USA, Silver Spring, MD), fitted with a guard column and connected in series to enable separation across the full size range of EPS. The mobile phase was a NaCl solution matching the ionic strength and pH of each corresponding adsorption experiment. The columns were calibrated using pullulan standards (2.0 mg $mL^{-1}$) of nominal molar mass 12.2, 48.0, 212, 380 and 863 kDa, and polydispersity values less than 1.2 (Polymer Laboratories, Silver Spring MD, US). Monomeric glucose was employed as a low molar mass (276 Da) standard. The injection volume and flow rate for all samples and standards were 100 μL and 1.0 mL $min^{-1}$, respectively. The Empower software program (Waters, Medford, MA) was used to determine peak area, and height, as well as weight—($M_w$) and number—($M_n$) averaged molar mass values. $M_w$ and $M_n$ were calculated according to:

$$M_w = \sum_{i=1}^{N} h_i(M_i) \Big/ \sum_{i=1}^{N} h_i, \quad (2)$$

$$M_n = \sum_{i=1}^{N} h_i \Big/ \sum_{i=1}^{N} (h_i/M_i), \quad (3)$$

where $h_i$ and $M_i$ are the height and molar mass, respectively, of the sample SE-HPLC curve at elution volume $i$.

### 2.7. FTIR spectroscopy

A Magna-IR 560 Nicolet spectrometer equipped with a CsI beam splitter, DTGS-detector and OMNIC processing software was used to record all spectra. For each sample, 350–400 scans were collected over the spectral range of 400–4000 $cm^{-1}$ at a resolution of 4 $cm^{-1}$. Aliquots of 100–1200 μL of supernatant solution were transferred onto IR transmissive Ge windows, dried under vacuum for 19 h, and spectra of EPS films were collected in transmission mode. Spectra of the freeze-dried solid phase were collected in diffuse reflectance (DRIFT) mode using a SpectraTech DRIFT accessory after gently mixing 10 mg of solid with 300 mg of IR grade KBr powder. Samples were then packed into in a stainless steel cup and scanned using pure KBr as background.

## 3. Results

The purified EPS isolated from *B. subtilis* was composed of 413, 80 and 30 g $kg^{-1}$ of carbon (EPS-C), nitrogen (EPS-N) and phosphorus (EPS-P), respectively. Protein and polysaccharide constituents dominate the EPS mass and occur at similar mass concentrations (Omoike and Chorover, 2004). Adsorption of EPS to Teflon tubes was negligible; recoveries of C, N and P from mineral-free controls were quantitative (>97%).

### 3.1. pH dependent adsorption of EPS-C, -N and -P

The mass fraction of goethite-adsorbed EPS-C, -N and -P decreases with increasing solution pH in 10 mM NaCl

(Fig. 1A). The fraction of P adsorbed exceeds that of both N and C at pH 3.2–7.5. At pH 3.2, the mean adsorbed quantities of EPS-C, -N and -P amount to 399 (±6), 87 (±2) and 40.3 (±0.2) μg $m^{-2}$, respectively. At pH 7.5, adsorbed C and N are 205 (±4), and 47.1 (±0.7) μg $m^{-2}$, respectively. As pH increases to 9.0 the fraction of adsorbed C exceeds that of N and P. Distribution coefficients ($K_d$) calculated for C, N and P as a function of solution pH illustrate the strong preferential adsorption of P-containing moieties at low pH and the steep decline in selective EPS-P uptake with increasing pH (Fig. 1B). The $K_d$ values for EPS-N and -C show less pH dependence, and at pH 9.1 the values are not different from those for EPS-P.

### 3.2. Effects of ionic strength (I)

The influence of $I$ on EPS adsorption to goethite was investigated by measuring EPS adsorption isotherms in 1,

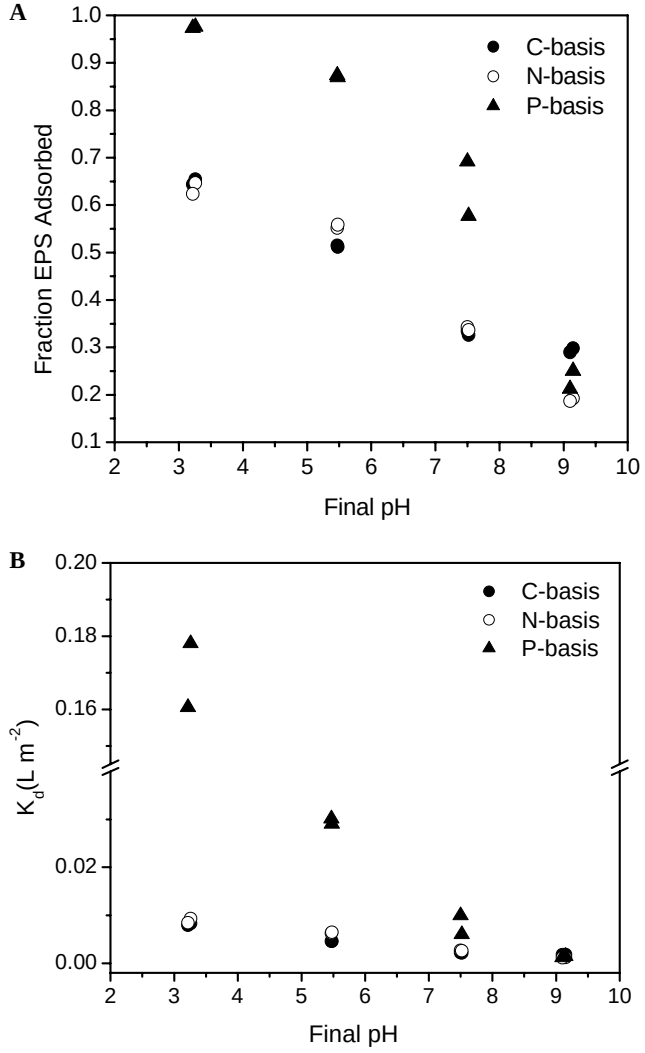


Fig. 1. (A) *Bacillus subtilis* EPS adsorption to goethite as a function of pH, (B) Variation in $K_d$ values of EPS constituents measured on the basis of carbon, nitrogen and phosphorus as a function of solution pH. Adsorption reaction was conducted at EPS-C concentration of 140 mg $L^{-1}$ in 10 mM NaCl electrolyte solution, $T = 23 \pm 2$ °C and 6 h.

10 and 100 mM NaCl background electrolyte solutions at pH 6.0. Adsorption isotherms plotted for EPS-C, -N and -P all show a decrease in EPS adsorption with increasing $I$ (Figs. 2A–C). The experimental data obtained for these curves were fitted to the linear form of Eq. (1), with $K$ and $\Gamma_{max}$ values determined from linear regression (Table 1). In the case of C and N, a good fit was generated throughout the concentration range using a single set of Langmuir parameters. In contrast, a two-term series of Langmuir equations (Sposito, 1984) was required to fit the full range of P adsorption data. The first equation (denoted by $P_1$ in Table 1), comprising high $K$ and low $\Gamma_{max}$, captures the high P adsorption at low aqueous concentration, whereas the second equation, with low $K$ and high $\Gamma_{max}$ (denoted by $P_2$ in Table 1) describes adsorption at higher loadings. Correlation coefficients ($r^2$) [0.951–0.997, 0.974–0.998 and 0.951–0.982 ($p < 0.001$) for EPS-C, EPS-N and EPS-P, respectively] indicate that the Langmuir models provide good empirical fits to the data, and they are plotted as lines in Fig. 2. Langmuir adsorption maxima ($\Gamma_{max}$) for EPS-N and EPS-$P_2$ are found to decrease with increasing $I$, whereas the adsorption maxima for EPS-$P_1$ were unaffected. $\Gamma_{max}$ values for EPS-C showed a decrease between 1 and 10 mM $I$ and no significant effect for $I > 10$ mM.

Distribution coefficient ($K_d$ values), where $K_d = \Gamma/C_e$, are plotted as a function of EPS-C concentration in Fig. 3. The data show a strong preference for adsorption of EPS-P relative to -N and -C, consistent with the much higher Langmuir $K$ values for EPS-P ($P_1$) in Table 1. $K_d$ values for EPS-P are typically an order of magnitude higher than those for EPS-C. Although $K_d$ for EPS-N and EPS-C are closer in value, preferential adsorption of N-containing moieties is apparent, particularly at higher [EPS]. Equilibrium solution pH increased from 6.0 to >7.0, in proportion to the mass of EPS adsorbed (Fig. 4) in the unbuffered suspensions.

### 3.3. Infrared spectra of adsorbed EPS

In the wavenumber region that is most useful for EPS infrared spectroscopy studies (2000–700 $cm^{-1}$), the DRIFT spectrum of unreacted goethite (Fig. 5a) shows two high frequency bands (1792 and 1662 $cm^{-1}$) corresponding to overtones of OH vibrations, and two low frequency bands located at 895 and 795 $cm^{-1}$ from Fe-OH in plane and out-of-plane bending vibrations, respectively (Ruan et al., 2001). DRIFT spectra of goethite after adsorption of EPS (Figs. 5b–e) show peaks at 1522 $cm^{-1}$ (amide II of proteins) and a broad sequence of peaks at 1200–950 $cm^{-1}$ (stretching vibrations of phosphodiesters and polysaccharides). A small band corresponding to symmetric stretching of $COO^-$ groups is observed at 1406 $cm^{-1}$ ($\nu_s$ $COO^-$), which may derive from proteins and carboxylated polysaccharides.

Fig. 6 shows DRIFT spectra of unreacted EPS (Fig. 6a) along with *difference spectra of EPS adsorbed to the goe-*

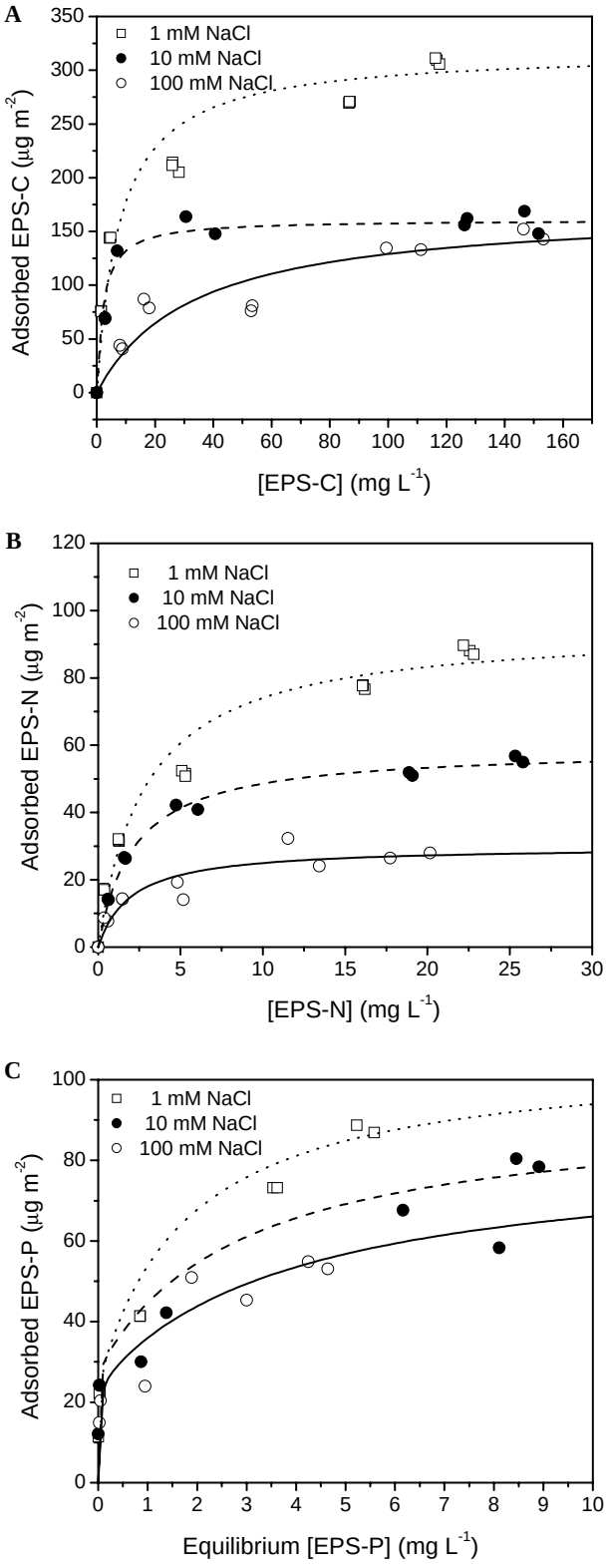


Fig. 2. Adsorption isotherms for *B. subtilis* EPS adsorption to goethite at pH 6 and varying ionic strength (1, 10 and 100 mM NaCl). (A) EPS-C, (B) EPS-N and (C) EPS-P. EPS-C concentration = 0–185 mg $L^{-1}$, Equilibration time = 6 h and $T = 23 \pm 2$ °C.

*thite surface* (Figs. 6b–e). The difference spectra were obtained by subtracting the goethite spectrum (Fig. 5a) from those of the goethite–EPS complex (Figs. 5b–e) and, therefore, they show only those bands resulting from the sorbed EPS. EPS spectral band assignments and associated references are summarized in Table 2. Clearly apparent in spectra of adsorbed EPS are the amide I (1680 $cm^{-1}$) and amide II (1520 $cm^{-1}$) bands associated with proteins, the symmetric stretching vibration of carboxylate (1406 $cm^{-1}$), polysaccharide vibrations (1100 $cm^{-1}$) and strong emergent bands that we have assigned to asymmetric (1263 $cm^{-1}$) and symmetric (1067 $cm^{-1}$) P=O stretching, O–P–O stretching (993 $cm^{-1}$), and P–O–Fe bonding (1153 and 1028 $cm^{-1}$). It should be noted that the putative phosphate bands exhibit some overlap with polysaccharide vibrations (Table 2).

### 3.4. Transmission spectra of aqueous-phase EPS

Transmission spectra of bulk EPS are shown in Fig. 7a, along with those of EPS remaining in solution following reaction with goethite, i.e., *sorption-fractionated* aqueous-phase EPS (Figs. 7b–d). The mass fractions of EPS removed from solution (by adsorption to goethite) in Fig. 7 are (a) 0, (b) 0.19, (c) 0.32 and (d) 0.48. Thus, Figs. 7a–d show the effects of an increasing extent of *sorptive fractionation* on the composition of EPS moieties remaining in solution. The spectra clearly show reduction in the intensities of amide (1800–1500 $cm^{-1}$) relative to polysaccharide vibrations (1250–950 $cm^{-1}$) with increasing mass fraction removed from solution. Loss of the intense 1078 $cm^{-1}$ vibration of sugar phosphate moieties is also observed, such that the broad and complex sugar phosphate/polysaccharide band absorbance is manifest at lower wavenumber.

### 3.5. Size fractionation of EPS species due to adsorption on goethite surface

The SE-HPLC unit was coupled to UV-photodiode array (PDA) and refractive index (RI) detectors in series to measure simultaneously UV-absorbing and non-UV-absorbing macromolecules in solution, before and after adsorption reaction with goethite. The PDA (top) and RI (bottom) chromatographic elution profiles of fractionated EPS at the three *I* are compared in Figs. 8A–C. The PDA data show chromophoric macromolecules (proteins and nucleic acids) only, while RI profiles include these constituents as well as non-chromophoric polysaccharides. The RI profiles show two major peaks corresponding to large (early elution) and small (late elution) macromolecules, respectively. The broad peak with low retention time corresponds with the only PDA signal, indicating that this peak in both data sets represents UV-absorbing protein and nucleic acid EPS constituents. The second peak at higher retention time in RI chromatograms does not appear in the PDA data and, therefore, reflects polysaccharide constituents.

The strong PDA peak at 10.47 min in the 1 mM NaCl supernatant (Fig. 8A) is absent in the UV profile of bulk EPS and goethite (EPS-free) supernatant solutions and it

Table 1
Langmuir constants calculated on C, N and P bases for adsorption of EPS to goethite (95% confidence intervals shown in parentheses)

| Ionic Strength (mM) | $\Gamma_m$ (μg m$^{-2}$) | | | | $K$ (L m$^{-2}$) | | | |
|---|---|---|---|---|---|---|---|---|
| | C | N | $P_1$ | $P_2$ | C | N | $P_1$ | $P_2$ |
| 1 | 315 (±9) | 95 (±3) | 24 (±4) | 82 (±5) | 0.126 (±0.031) | 0.352 (±0.006) | 302 (±12) | 0.56 (±0.063) |
| 10 | 161 (±4) | 59 (±1) | 28 (±5) | 65 (±4) | 0.458 (±0.003) | 0.47 (±0.06) | 327 (±24) | 0.34 (±0.081) |
| 100 | 172 (±18) | 30 (±2) | 25 (±5) | 60 (±5) | 0.03 (±0.01) | 0.5 (±0.2) | 64 (±8) | 0.25 (±0.1) |

A two-term series of Langmuir equations was best fit to the P adsorption data, yielding $\Gamma_m$ and $K$ parameters for low ($P_1$) and high ($P_2$) surface loadings, respectively.

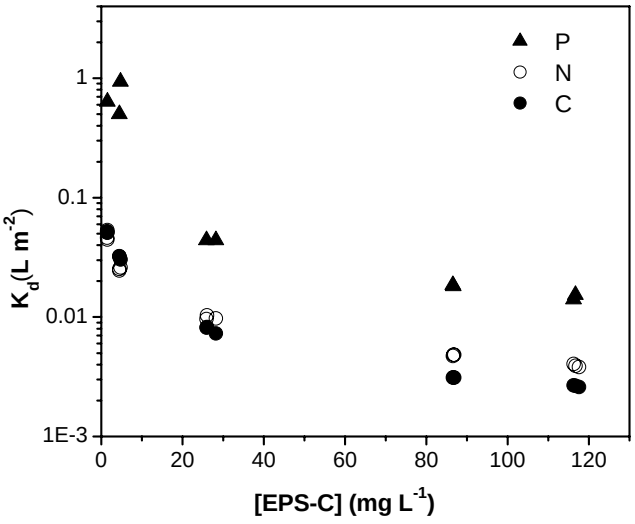


Fig. 3. Variation in $K_d$ values of EPS on the basis of C, N and P as a function of [EPS-C] at end of reaction in 1.0 mM NaCl at pH 6.0 and 6 h. EPS-C concentration = 0–185 mg L$^{-1}$ and $T = 23 \pm 2$ °C.

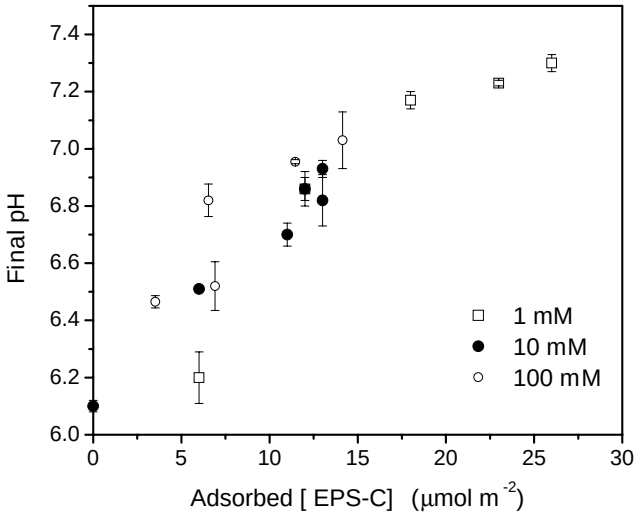


Fig. 4. Variation in solution pH after 6 h reaction time as a function of adsorbed EPS-C at ionic strengths of 1, 10 and 100 mM NaCl. EPS-C concentration = 0–185 mg L$^{-1}$ and $T = 23 \pm 2$ °C.

is also not observed in the SE-HPLC profiles for the 10 and 100 mM supernatant solutions. ICP-MS (Fe) and UV–vis analysis of the solutions from the 1 mM $I$ systems revealed that this 10.47 min peak results from micro-colloidal goethite that is stabilized in suspension by EPS sorption at

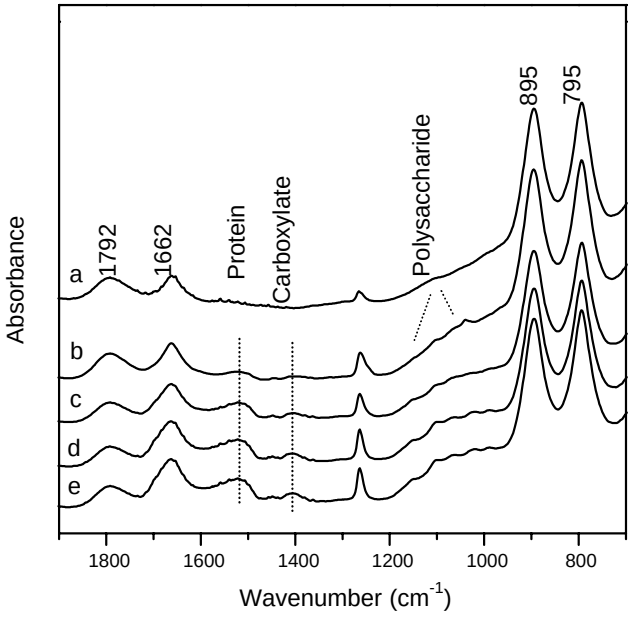


Fig. 5. DRIFT spectra of (a) goethite (before reaction with EPS) and (b–e) goethite–EPS complexes after reaction. Surface C loadings are (b) 0.076, (c) 0.144, (d) 0.270 and (e) 0.309 mg m$^{-2}$. Adsorption experiments were conducted in 1 mM NaCl and at pH 6.0.

low ionic strength. These suspended particles comprise less than 1% of the initial goethite concentration. Two of the 100 mM RI profiles at lower EPS-C concentration (111 and 53 mg L$^{-1}$) show negative peaks at an elution time of 21.3 min immediately following the positive polysaccharide peaks. These *system* peaks are most likely the result of solvent vacancy caused by sample injection, which is known to alter the refractive index of the mobile phase (Slais and Krejci, 1974; Shibukawa, 1995). Vacancy peaks were observed consistently when low [EPS] (including unreacted) solutions were injected under conditions of high $I$ for SE-HPLC analysis (data not shown). The vacancy peaks appear only in RI profiles because they reflect changes in linear velocity between UV-transparent solvent and EPS macromolecules in the column.

With increasing fraction of adsorbed EPS, the retention times of PDA and RI protein peaks are both shifted to increased retention time, indicating the preferential removal from solution of high molecular weight EPS constituents. To provide a semi-quantitative measure of changes in mean molar mass resulting from adsorption, the RI data were

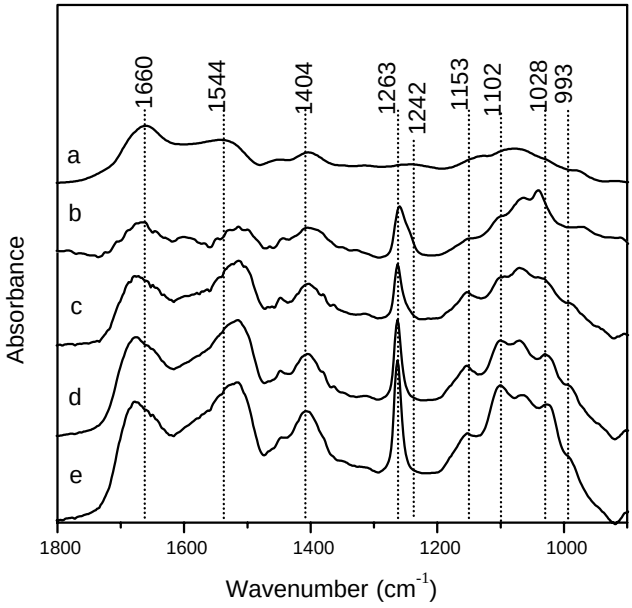


Fig. 6. (a) DRIFT spectrum of bulk EPS (no contact with goethite) and (b–e) DRIFT difference spectra of goethite-sorbed EPS with C adsorbed at (b) 0.076, (c) 0.144, (d) 0.270 and (e) 0.309 mg $m^{-2}$. Difference spectra were obtained by subtracting the goethite spectrum (Fig. 5a) from those of the goethite–EPS complexes. Adsorption reactions were conducted in 1 mM NaCl at pH 6.

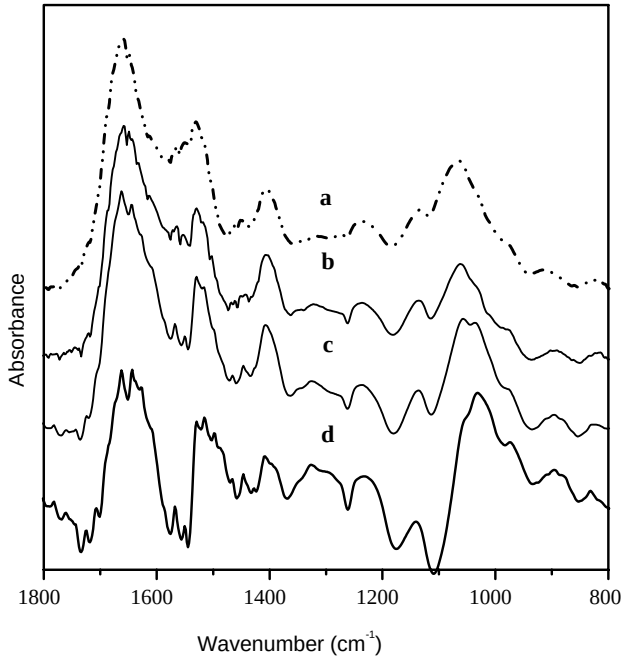


Fig. 7. Transmission spectra of EPS solution films dried on an IR transmissive (Ge) window. (a) Bulk EPS solution (no contact with goethite), and (b–d) EPS equilibrium supernatant solutions after adsorption from solution of (b) 19%, (c) 32% and (d) 48% of EPS-C. Adsorption reactions were conducted in 10 mM NaCl at pH 6.0.

Table 2
Band assignments[a] for DRIFT (Fig. 6) and transmission (Fig. 7) spectra of EPS before and after sorption to goethite

| Vibration frequencies ($cm^{-1}$) | | Band assignments |
|---|---|---|
| EPS (bulk) | Goethite-sorbed EPS [0.309 (mg $m^{-2}$ C)] | |
| 1660 | 1677 | $\nu$ C═O of amides associated with proteins (amide I) |
| 1544 | 1516 | $\delta$ N–H and $\nu$ C–N in –CO-NH– of proteins (amide II) |
| 1449 | 1447 | $\delta_s$ $CH_2$, and $\delta$ C–OH |
| 1404 | 1406 | $\nu_s$ C–O of $COO^-$ groups |
| 1242 | 1263 | $\nu_{as}$ P═O of phosphodiester backbone of nucleic acid (DNA and RNA); may also be due to phosphorylated proteins |
| | 1153 | $\nu$ P–O–Fe |
| 1127 | 1102 | O–H deformation, $\nu$ C–O, ring vibrations of polysaccharides |
| 1078 | 1067 | $\nu_s$ P═O of phosphodiester backbone of nucleic acid (DNA and RNA), C–O–C and C–O–P. Also phosphorylated proteins and C–OH stretch. |
| | 1028 | $\nu$ P–O–Fe |
| 920 | 993 | Asymmetric ester O–P–O stretching modes from nucleic acids |

$\nu_s$, symmetric stretch; $\nu_{as}$, asymmetric stretch; $\delta_s$, symmetric deformation (bend); $\delta_s$, symmetric deformation (bend).

[a] Band assignments from Fringeli and Günthard (1981), Tejedor-Tejedor and Anderson (1990), Zeroual et al. (1994), Persson et al. (1996), Naumann et al. (1996), Barja et al. (1999), Gue et al. (2001), Sheals et al. (2002), Omoike and Chorover (2004), Omoike et al. (2004).

calibrated against pullulan standards for determination of *apparent* weight-average and number-average molar masses ($M_w$ and $M_n$, respectively) of solution phase EPS as a function of adsorbed fraction. As shown in Table 3, the apparent $M_n$ and $M_w$ of sorption-fractionated EPS solutions decrease with increasing fraction of EPS adsorbed by goethite particles.

As indicated by comparison of the two principal RI chromatogram peaks, the data also show a relative decrease in peak intensity for the early eluting "protein" peak compared to the later eluting "polysaccharide" peak (Fig. 8B). Fractionation of EPS because of preferential protein adsorption was estimated from the ratio of peak areas and heights for the protein and polysaccharide constituents. The peak area and height ratios are reported as the "fractionation indices", $F_A$ and $F_H$, respectively (Table 4). All $F$ values are found to decrease following reaction with goethite, indicating the preferential adsorption of proteinaceous relative to polysaccharide constituents. For the 100 mM $I$ case, the vacancy peaks at 21.3 min for the two lowest EPS-C concentrations (53 and 11 mg $L^{-1}$) overlap with the polysaccharide peak, diminishing its true

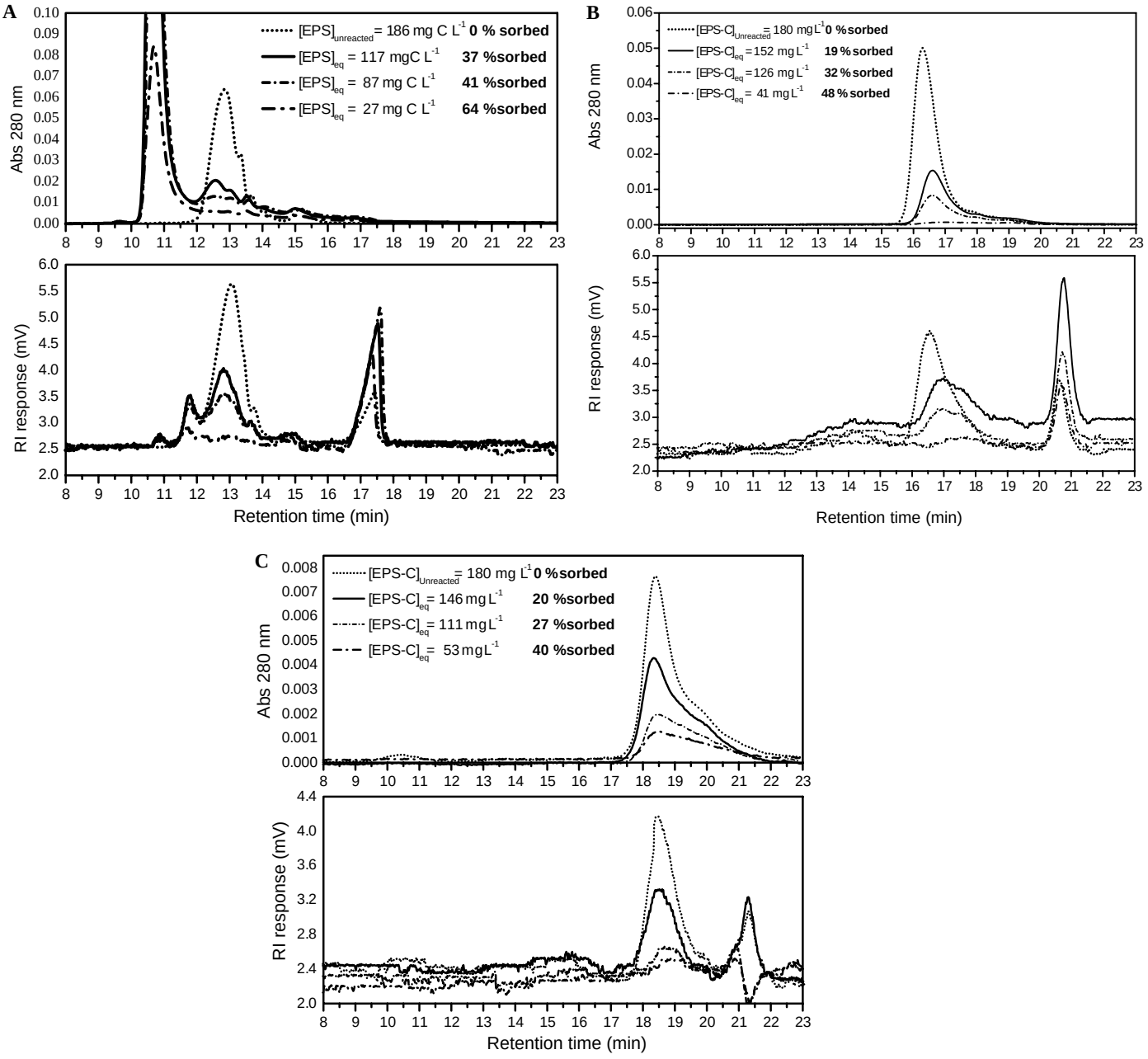


Fig. 8. SE-HPLC elution profiles for EPS solutions before and after reaction with goethite at pH 6 in NaCl background solutions of variable ionic strength: (A) 1 mM, (B) 10 mM and (C) 100 mM. Top: UV elution profile (absorbance measured at 280 nm); bottom: RI elution.

height and area, making it impossible to determine an accurate $F$ value for those two cases.

## 4. Discussion

### 4.1. Effects of solution pH

Changes in solution chemistry impact ionizable functional groups on both EPS and goethite, which has implications for the adsorption reaction. EPS functional groups are mostly protonated at pH < 2, but become progressively negative-charged with increasing pH due to proton dissociation of carboxyl [pH 2.0–6.0], phospholipid [pH 2.4–7.2], phosphodiester [pH 3.2–3.5], hydroxyl [pH 9.0–10.0] and amino [pH 9.0–11.0] groups (Martinez et al., 2002). Likewise, proton adsorption and desorption at goethite surface hydroxyl groups exhibits strong pH dependence. The point of zero net proton charge (PZNPC) of the synthetic goethite particles is between 7.2 and 8.0 (Day et al., 1994; Stumm and Morgan, 1996). Adsorption of EPS constituents should, therefore, be favorable electrostatically at pH < PZNPC where goethite and EPS are oppositely charged. The mass of EPS adsorbed (C, N or P basis, Fig. 1) decreased significantly with increasing pH. Similar pH dependency has been reported in goethite adsorption studies of natural organic matter (NOM) and

Table 3
Apparent molecular mass distribution data for solution phase EPS constituents before and after reaction with goethite in 10 and 100 mM NaCl at pH 6

| EPS sorbed (%) | Retention time (min) | Molecular weight (kDa) | | Polydispersity ($M_w/M_n$) |
|---|---|---|---|---|
| | | $M_n$ [a] | $M_w$ [b] | |
| 10 mM | | | | |
| 0 | 16.48 | 11530 ± 2124 | 14619 ± 1613 | 1.28 ± 0.095 |
| 18 | 16.71 | 9118 ± 2365 | 12579 ± 2770 | 1.34 ± 0.126 |
| 33 | 16.89 | 8873 ± 760 | 10550 ± 490 | 1.33 ± 0.25 |
| 45[c] | | | | |
| 0 | 20. 63 | 668 ± 5.77 | 689 ± 8.08 | 1.03 ± 0 |
| 18 | 20. 67 | 643 ± 39.63 | 660 ± 43.59 | 1.03 ± 0.01 |
| 33 | 20.73 | 623 ± 5.48 | 634 ± 2.87 | 1.02 ± 0.01 |
| 45 | 20.72 | 631 ± 7.59 | 643 ± 5.85 | 1.02 ± 0 |
| 100 mM | | | | |
| 0 | 18.50 | 2234 ± 169 | 2576 ± 47 | 1.15 ± 0.034 |
| 20 | 18.60 | 2158 ± 144 | 2537 ± 84 | 1.18 ± 0.059 |
| 27 | 18.70 | 1893 ± 159 | 2261 ± 127 | 1.20 ± 0.057 |
| 40 | 18.80 | 1774 ± 404 | 1983 ± 318 | 1.13 ± 0.077 |
| 0 | 21.30 | 230 ± 8.89 | 242 ± 6.54 | 1.04 ± 0.023 |
| 20 | 21.00 | 294 ± 53.98 | 305 ± 49.09 | 1.06 ± 0.017 |
| 27 | 20.80 | 361 ± 24 | 376 ± 35 | 1.04 ± 0.029 |
| 40 | 20.80 | 364 ± 12.75 | 375 ± 14.5 | 1.03 ± 0.003 |

Derived from refractive index detector data.
[a] Number average molecular weight calculated according to Eq. (3).
[b] Weight average molecular weight calculated according to Eq. (2).
[c] Signal too low for mass parameter quantification.

Table 4
SE-HPLC fractionation results for batch adsorption studies of *B. subtilis* EPS on goethite at different ionic strengths

| 1 mM | | 10 mM | | 100 mM | |
|---|---|---|---|---|---|
| % C sorbed | $F_A$ [a] (±SD) | % C sorbed | $F_A$ [a] (±SD) | % C sorbed | $F_A$ [a] (±SD) |
| 0 | 6 ± 1.3 | 0 | 3.6 ± 0.8 | 0 | 3.4 ± 0.4 |
| 37 | 1.6 ± 0.4 | 19 | 1.6 ± 0.3 | 20 | 1.7 ± 0.06 |
| 41 | 1.5 ± 0.3 | 32 | 1.5 ± 0.3 | 27 | ND |
| 64 | 0.6 ± 0.1 | 48 | 0.3 ± 0.1 | 40 | ND |
| 1 mM | | 10 mM | | 100 mM | |
| % C sorbed | $F_H$ [b] (± SD) | % C sorbed | $F_H$ [b] (± SD) | % C sorbed | $F_H$ [b] (± SD) |
| 0 | 2.9 ± 0.1 | 0 | 1.6 ± 0.2 | 0 | 2.1 ± 0.09 |
| 37 | 0.6 ± 0.09 | 19 | 0.5 ± 0.1 | 20 | 1.0 ± 0.02 |
| 41 | 0.4 ± 0.06 | 32 | 0.6 ± 0.2 | 27 | ND |
| 64 | 0.2 ± 0.02 | 48 | 0.1 ± 0.03 | 40 | ND |

Calculations based on both area ($F_A$) and height ($F_H$) of chromatographic peaks for solution phase EPS before and after adsorption reaction. ND, not determined due to vacancy peak overlap.
[a] $F_A$ = protein peak ($A_p$): polysaccharide ($A_{ps}$) peak height ratio.
[b] $F_H$ = protein ($H_p$): polysaccharide ($H_{ps}$) peak area ratio.

low molar mass organic acids (Davis, 1982; Murphy et al., 1992; Evanko and Dzombak, 1998). The adsorption of biomacromolecules such as proteins and charged polysaccharides has also been reported to decrease with increasing pH (Revilla et al., 1996; Jones and O'Melia, 2000; Fujimoto and Petri, 2001). However, in the case of proteins, adsorption maxima tend to occur at pH close to the isoelectric point of the protein (Revilla et al., 1996; Jones and O'Melia, 2000). The pH dependency of EPS-P adsorption reported here is also consistent with prior studies of inorganic and organic phosphate sorption (decreased adsorption with increasing pH) to goethite (Geelhoed et al., 1997; Nowack and Stone, 1999).

### 4.2. Screening-reduced adsorption

At pH 6, adsorption of poly-anionic EPS-C and -N to the positive-charged goethite surface was found to decrease with increasing $I$ (Fig. 2, Table 1). This trend is in contrast to studies of humic substances, which showed either *increased* adsorption with increasing $I$ (Lafrance and Mazet, 1989) or negligible $I$ effect (Jardine et al., 1989; Gu et al., 1994). Increased adsorption at high electrolyte concentration may be attributed to higher surface charge at a given pH (Dzombak and Morel, 1990). In contrast, our data are more consistent with trends reported for protein adsorption via ion exchange (Lan et al., 2001). Indeed, the source of N in our sample is dominantly proteins and smaller amounts of nucleic acids (Omoike and Chorover, 2004). The decrease in $\Gamma_{max}$ for EPS-N with increasing $I$ (Table 1) is similar to that reported for protein adsorption on a range of surfaces including cation and anion exchangers and dye-affinity adsorbents (Hashim et al., 1995; Lan et al., 2001). In addition, the Langmuir constant, $K$, obtained in those studies increased with increasing $I$, a trend consistent with the $K$ values for N in our study (Table 1). Increasing $I$ was also reported to diminish adsorption of dextran, a neutral polysaccharide, on $TiO_2$ (anatase), the reduction being attributed to disruption of surface H-bonding because of counter-ion $Cl^-$ adsorption (Li and Spencer, 1992). According to numerical calculations by Vandesteeg et al. (1992), polyelectrolyte adsorption at opposite-charged surfaces includes two regimes: (i) *screening-reduced adsorption*, characterized by decreasing adsorbed mass with increasing $I$ and (ii) *screening-enhanced adsorption* characterized by increasing adsorbed amount with increasing $I$.

Strong negative $I$ dependence of polymer adsorption has been attributed to electrostatic mechanisms of surface interaction (Hesselink, 1977; Vandesteeg et al., 1992). In particular, increased competition from counter-ions in the background electrolyte lead to a reduction in EPS adsorption. Counter-ions can bind to functional groups of EPS (Fleer et al., 1993) as well as the surface hydroxyl groups of goethite (Bajpai et al., 1997). The competitive effects of background electrolyte are likely to be enhanced at high $I$. Specifically, adsorption of $Cl^-$ to the goethite surface and of $Na^+$ to EPS in bulk solution are both expected to diminish EPS electrostatic adsorption to goethite because of charge screening (if ion sorption is diffuse or outer-sphere) or neutralization (if ion sorption results from inner-sphere complexation). Additional factors that could

contribute to the negative *I* effect are contraction in EPS conformation (Frank and Belfort, 1997) and increased goethite homo-coagulation at high electrolyte concentration (Anderson et al., 1985), since these processes would reduce the number of reactive sites on the adsorptive and adsorbent, respectively.

### 4.3. Infrared evidence for phosphate group ligand exchange

The observed $OH^-$ release (Fig. 4), DRIFT data (Figs. 5 and 6), and our prior ATR-FTIR studies (Omoike et al., 2004) argue against strictly Coulombic adsorption of EPS at the goethite surface. The positive relation between EPS adsorption and $OH^-$ release is consistent with a ligand exchange mechanism that results in displacement of goethite surface hydroxyls during binding of EPS functional groups to surface metal (Fe) centers. Such pH effects have been reported previously to coincide with adsorption of NOM, low molecular weight organic acids or orthophosphate onto mineral oxides (Kummert and Stumm, 1980; Davis, 1982). Specifically, these prior studies have emphasized the formation of inner-sphere carboxylate-Fe bonds and phosphate-Fe bonds during NOM and orthophosphate adsorption, respectively. These molecular mechanisms have been verified via infrared spectroscopy (Gu et al., 1994; Persson et al., 1996; Chorover and Amistadi, 2001).

In contrast to reports on carboxylated humic matter, infrared (DRIFT) spectra of free and adsorbed EPS (Fig. 6) show no change in the frequency of the symmetric carboxylate stretch ($\nu_{sym}$ $COO^-$, ca. 1405 $cm^{-1}$) upon adsorption. Thus, covalent bonding of carboxylate groups to the goethite surface was not detected by DRIFT. However, comparison of the bulk EPS spectrum with difference spectra of goethite-sorbed EPS showed significant differences in the protein (1700–1500 $cm^{-1}$) and polysaccharide (1200–950 $cm^{-1}$) regions, indicating EPS perturbation due to the surface reaction.

The 1200–950 $cm^{-1}$ region is characterized by C–O–C, C–O–P, P–O–P and C–O stretching vibrations of polysaccharides [sugars/sugar phosphates] as well as phosphodiesters ($PO_2^-$) (Fringeli and Günthard, 1981; Naumann et al., 1996; Naumann, 2000). Changes in the frequency of bands assigned to $\nu_{as}$ $PO_2^-$ and $\nu_s$ $PO_2^-$ are evident in Figs. 6b–e. The $\nu_{as}$ $PO_2^-$ located at 1242 $cm^{-1}$ in the spectrum of bulk EPS, is shifted to 1263 $cm^{-1}$, while peak absorbance for the broad $\nu_s$ $PO_2^-$ band is apparently shifted from 1078 to 1067 $cm^{-1}$ (Table 2). Most important is the emergence of two new bands, located at 1153 and 1028 $cm^{-1}$ in Figs. 6b–e (absent in Fig. 6a), that are consistent with stretching vibrations of P–O–Fe bonds as indicated by both empirical and molecular modeling studies (Tejedor-Tejedor and Anderson, 1990; Barja et al., 1999; Gong, 2001; Sheals et al., 2002; Omoike et al., 2004). Emergence of these two new bands and the associated shifts in $\nu_{as}$ $PO_2^-$ and $\nu_s$ $PO_2^-$ are consistent with inner-sphere bonding of EPS phosphate groups (deriving principally from phosphodiesters of nucleic acids and proteins) at goethite surface hydroxyls. This ligand exchange mechanism provides an intriguing explanation for both $OH^-$ release (Fig. 4) and the high EPS-P affinity (Table 1, Figs. 2C, and 3). The strong pH dependence of EPS-P adsorption relative to that for –N and –C (Fig. 1B) may reflect the greater favorability of the ligand exchange reaction at low pH where goethite surface hydroxyls are protonated and, therefore, more exchangeable with EPS phosphate groups.

### 4.4. Infrared evidence for preferential protein adsorption

Protein adsorption is indicated by the presence of amide I and II vibrations in sorbed EPS (Fig. 6). Relative to bulk EPS, these two bands are shifted to higher and lower frequencies, respectively, upon goethite-surface reaction. In addition, adsorbed EPS shows a reduction in amide I/amide II intensity ratio (Fig. 6). Increased relative intensity of the amide II peak at ca. 1516 $cm^{-1}$ coincides with increasing EPS adsorption to the goethite surface. Both peak and integrated intensities of this band have been used to measure the extent of protein adsorption onto surfaces (Schakenraad and Busscher, 1989; Roddick-Lanzilotta et al., 1998). Peak absorbance data for the amide II band as a function of [EPS-N] were fitted to a modified version of the Langmuir equation developed for IR spectroscopic application (Roddick-Lanzilotta et al., 1998). A plot of $[EPS\text{-}N]_{eq}/Abs(1516\ cm^{-1})$ vs $[EPS\text{-}N]_{eq}$ (analogous to the linearized form of Eq. (1)) gave a slope of $8.90 \pm 0.4$ and an intercept of $9.74\ (\pm 3.9) \times 10^{-4}$, respectively. The ratio of slope to intercept, which provides an estimate of the Langmuir constant (*K*) for EPS proteins, was $9.1\ (\pm 3.6) \times 10^3$ L $mol^{-1}$. This is within the range ($3 \times 10^3$–$6 \times 10^4$ L $mol^{-1}$) reported for adsorption of lysine peptides and polylysine on $TiO_2$ (Roddick-Lanzilotta et al., 1998).

Enhancement of amide vibrations in DRIFT spectra for solid phase products is corroborated by inverse trends in transmission spectra of the solution phase EPS (Fig. 7). That is, both sets of IR data indicate that with increasing adsorbed fraction of EPS, the solution phase becomes relatively enriched in polysaccharides, whereas the goethite surface becomes relatively enriched in proteins. The dual-detector SE-HPLC results (Fig. 8) are also consistent with this finding; they too indicate preferential adsorption of UV-absorbing proteins and nucleic acids relative to polysaccharides. In addition, the SE-HPLC data reveal selective adsorption of those proteins with higher molar mass. Adsorptive uptake of high molar mass fractions has also been reported in prior SE-HPLC studies of NOM adsorption to Fe oxide surfaces (Tomaic and Zutic, 1988; Meier et al., 1999; Zhou et al., 2001; Chorover and Amistadi, 2001).

## 5. Conclusions

Since bacterial EPS is a heterogeneous mixture of biomacromolecules, each one comprising a multiplicity of functional groups, it is expected that numerous mechanisms influence

its adsorption to mineral surfaces. A multi-faceted experimental approach is, therefore, required to elucidate these interactions. Adsorption of EPS-C, -N and -P decreases with increasing pH from 3 to 9 because of progressive proton dissociation of both goethite and ionizable EPS functional groups. The pH dependency of EPS-P adsorption exceeds that of C and N. At pH $< 9$ (pH $<$ PZNPC of goethite), element specific $K_d$ values reflect preferential uptake of P and N containing moieties (i.e., $K_d$ values follow the order EPS-P $\gg$ EPS-N $>$ EPS-C).

At pH 6, decreased adsorption with increasing ionic strength is consistent with screening-reduced electrostatic interactions between polyanionic EPS and the positive-charged goethite surface. Infrared spectroscopy indicates that, in addition to Coulombic attraction, EPS adsorption results in the formation of P–O–Fe bonds between phosphoryl groups and goethite-surface Fe metal centers. This ligand exchange reaction, which results in the release to solution of goethite surface hydroxyls and a corresponding increase in solution pH, provides explanation for the strong preferential adsorption of EPS-P, relative to –C and –N. A similar ligand exchange reaction involving EPS carboxyl groups was not observed. Several lines of evidence, including infrared spectroscopy, elemental analysis and dual-mode-detection SE-HPLC indicate preferential uptake of proteins and nucleic acids relative to polysaccharides. Nucleic acids and proteins—adsorbed via both inner-sphere and electrostatic adsorption mechanisms—therefore likely play an important role in conditioning film formation and bacterial adhesion to Fe oxide surfaces.

## Acknowledgments

The authors are grateful to Mary-Kay Amistadi for her assistance with phosphorus and iron analysis by ICP-MS. The helpful comments of Patricia Maurice, AE Nagy, and two anonymous reviewers are appreciated. This research was supported by the National Science Foundation (NSF) CRAEMS program (Grant CHE-0089156).

*Associate editor:* Kathryn L. Nagy

## References

An, Y.H., Friedman, R.J., 1998. Concise review of mechanisms of bacterial adhesion to biomaterial surfaces. *J. Biomed. Mater. Res.* **43**, 338–348.

Anderson, M.A., Tejedor-Tejedor, M.I., Stanforth, R.R., 1985. Influence of aggregation on the uptake kinetics of phosphate by goethite. *Environ. Sci. Technol.* **19**, 632–637.

Atkinson, R.J., Posner, A.M., Quirk, J.P., 1967. Adsorption of potential-determining ions at ferric oxide-aqueous electrolyte interface. *J. Phys. Chem.* **71**, 550–558.

Bajpai, A.K., Rajpoot, D.D., Mishra, D.D., 1997. Studies on the adsorption of sulfapyridine at the solution-alumina interface. *J. Colloid Interface Sci.* **187**, 96–104.

Barja, B.C., Tejedor-Tejedor, M.I., Anderson, M.A., 1999. Complexation of methylphosphonic acid with the surface of goethite particles in aqueous solution. *Langmuir* **15**, 2316–2321.

Bos, R., van der Mei, H.C., Busscher, H.J., 1999. Physico-chemistry of initial microbial adhesive interactions—its mechanisms and methods for study. *FEMS Microbiol. Rev.* **23**, 179–229.

Bradshaw, D.J., Marsh, P.D., Watson, G.K., Allison, C., 1997. Effect of conditioning films on oral microbial biofilm development. *Biofouling* **11**, 217–226.

Charaklis, W.G., 1990. In: Charaklis, W.G. Marshall, K.C. (Eds.), *Biofilms*, Wiley, New York, pp. 195–231.

Chorover, J., Amistadi, M.K., 2001. Reaction of forest floor organic matter at goethite, birnessite and smectite surfaces. *Geochim. Cosmochim. Acta* **65**, 95–109.

Davies, D.G., Chakrabarty, A.M., Geesey, G.G., 1993. Exopolysaccharide production in biofilms: substratum activation of alginate gene expression by *Pseudomonas aeruginosa*. *Appl. Environ. Microbiol.* **59**, 1181–1186.

Davis, J.A., 1982. Adsorption of natural dissolved organic matter at the oxide/water interface. *Geochim. Cosmochim. Acta* **46**, 2381–2393.

Day, G.M., Hart, B.T., McKelvie, I.D., Beckett, R., 1994. Adsorption of natural organic matter onto goethite. *Colloid Surf. A: Phys. Engin. Aspects* **89**, 1–13.

de Brouwer, J.F.C., Wolfstein, K., Stal, L.J., 2002. Physical characterization and diel dynamics of different fractions of extracellular polysaccharides in an axenic culture of a benthic diatom. *Eur. J. Phycol.* **37**, 37–44.

Dzombak, D.A., Morel, F.M.M., 1990. *Surface Complexation Modeling: Hydrous Ferric Oxide*. John Wiley and Sons, NY.

Evanko, C.R., Dzombak, D.A., 1998. Influence of structural features on sorption of NOM-analogue organic acids to geothite. *Environ. Sci. Technol.* **32**, 2846–2855.

Fleer, G.J., Cohen, M.A., Stuart, J.M., Scheutjens, T., Cosgrove, B., 1993. *Polymers at Interfaces*. Chapman and Hall, London, p. 502.

Frank, B.P., Belfort, G., 1997. Intermolecular forces between extracellular polysaccharides measured using the atomic force microscope. *Langmuir* **13**, 6234–6240.

Fringeli, U.P., Günthard, H.H., 1981. Infrared membrane spectroscopy. In: Grell, E. (Ed.), *Membrane Spectroscopy*. Springer-Verlag, Berlin, pp. 270–332.

Fujimoto, J., Petri, D.F.S., 2001. Adsorption behavior of carboxymethylcellulose on amino-terminated surfaces. *Langmuir* **17**, 56–60.

Geelhoed, J.S., Hiemstra, T., VanRiemsdijk, W.H., 1997. Phosphate and sulfate adsorption on goethite: single anion and competitive adsorption. *Geochim. Cosmochim. Acta* **61**, 2389–2396.

Gong, W., 2001. A real time in situ ATR-FTIR spectroscopic study of linear phosphate adsorption on titania surfaces. *Int. J. Miner. Process.* **63**, 147–165.

Gu, B.H., Schmitt, J., Chen, Z.H., Liang, L.Y., McCarthy, J.F., 1994. Adsorption and desorption of natural organic matter on iron oxide: mechanisms and models. *Environ. Sci. Technol.* **28**, 38–46.

Gubner, R., Beech, I.B., 2000. The effect of extracellular polymeric substances on the attachment of *Pseudomonas* NCIMB 2021 to AISI 304 and 316 stainless steel. *Biofouling* **15**, 25–36.

Gue, M., Dupont, V., Dufour, A., Olivier, S., 2001. Bacterial swarming: a biochemical time-resolved FTIR-ATR study of *Proteus mirabilis* swarm cell differentiation. *Biochemistry* **40**, 11938–11945.

Hashim, M.A., Chu, K., Tsan, P.S., 1995. Effects of ionic strength and pH on the adsorption equilibria of lysozyme on ion exchangers. *J. Chem. Technol. Biotechnol.* **62**, 253–260.

Hesselink, F.T., 1977. Theory of polyelectrolyte adsorption—effect on adsorption behavior of electrostatic contribution to adsorption free energy. *J. Colloid Interface Sci.* **60**, 448–466.

Jardine, P.M., Weber, N.L., McCarthy, J.F., 1989. Mechanisms of dissolved organic-carbon adsorption on soil. *Soil Sci. Soc. Am. J.* **53**, 1378–1385.

Jones, K.L., O'Melia, C.R., 2000. Protein and humic acid adsorption onto hydrophilic membrane surfaces: effects of pH and ionic strength. *J. Membrane Sci.* **165**, 31–46.

Kummert, R., Stumm, W., 1980. The surface complexation of organic acids on hydrous $\gamma$-$Al_2O_3$. *J. Colloid Interface Sci.* **75**, 373–385.

Lafrance, P., Mazet, M., 1989. Adsorption of humics substances in the presence of sodium salts. *J. Am. Water Works Assoc.* **81**, 155–162.

Lan, Q.D., Bassi, A.S., Zhu, J.X., Margaritis, A., 2001. A modified Langmuir model for the prediction of the effects of ionic strength on the equilibrium characteristics of protein adsorption onto ion exchange/affinity adsorbents. *Chem. Engin. J.* **81**, 179–186.

Li, Y., Spencer, H.G., 1992. Adsorption of dextrans on spherical $TiO_2$ particles. *Colloid Surface* **66**, 89–195.

Meier, M., Namjesnik-Dejanovic, K., Maurice, P.A., Chin, Y.-P., Aiken, G.R., 1999. Fractionation of aquatic natural organic matter upon sorption to goethite and kaolinite. *Chem. Geol.* **157**, 275–284.

Martinez, R.E., Smith, D.S., Kulczycki, E., Ferris, F.G., 2002. Determination of intrinsic bacterial surface acidity constants using a Donnan shell model and a continuous $pK_a$ distribution method. *J. Colloid Interface Sci.* **253**, 130–139.

Murphy, E.M., Zachara, J.M., Smith, S.C., Phillips, J.L., 1992. The sorption of humic acids to mineral surfaces and their role in contaminant binding. *Sci. Tot. Environ.* **118**, 413–423.

Naumann, D., Schultz, C.P., Helm, D., 1996. What can infrared spectroscopy tell us about the structure and composition of intact bacterial cells? In: Mantsch H.H., Chapman, D. (Eds.), *Infrared Spectroscopy of Biomolecules*. Wiley-Liss Inc., New York, pp. 279–310, Chapter 10.

Naumann, D., 2000. FT-Infrared and FT-Raman spectroscopy in biomedical research. In: Gremlich, H., Yan, B. (Eds.), *Infrared and Raman Spectroscopy of Biological Materials*. Marcel Dekker Inc., New York, p. 323.

Neu, T.R., 1996. Significance of bacterial surface-active compounds in interaction of bacteria with interfaces. *Microbiol. Rev.* **60**, 151–166.

Nowack, B., Stone, A.T., 1999. Adsorption of phosphonates onto the goethite-water interface. *J. Colloid Interface Sci.* **214**, 20–30.

Omoike, A., Chorover, J., 2004. Spectroscopic study of extracellular polymeric substances from *Bacillus subtilis*: aqueous chemistry and adsorption effects. *Biomacromolecules* **5**, 1219–1230.

Omoike, A., Chorover, J., Kwon, K., Kubicki, J., 2004. Adhesion of bacterial exopolymers to alpha-FeOOH: inner-sphere complexation of phosphodiester groups. *Langmuir* **20**, 11108–11114.

Persson, P., Nilsson, N., Sjöberg, S., 1996. Structure and bonding of orthophosphate ions at the iron oxide-aqueous interface. *J. Colloid Interface Sci.* **177**, 263–275.

Revilla, J., Eloisa, A., Carrier, P., Picot, C., 1996. Adsorption of bovine serum albumin onto polystyrene latex particles bearing saccharidic moieties. *J. Colloid Interface Sci.* **180**, 405–412.

Roddick-Lanzilotta, A.D., Connor, P.A., McQuillan, A.J., 1998. An in situ infrared spectroscopic study of the adsorption of lysine to $TiO_2$ from an aqueous solution. *Langmuir* **14**, 6479–6484.

Ruan, H.D., Frost, R.L., Kloprogge, J.T., 2001. The behavior of hydroxyl units of synthetic goethite and its dehydroxylated product hematite. *Spectrochim. Acta A* **57**, 2575–2586.

Schakenraad, J.M., Busscher, H.J., 1989. Cell-polymer interactions: the influence of protein adsorption. *Colloid Surface* **42**, 331–343.

Scharfman, A., Degroote, S., Beau, J., Lamblin, G., Roussel, P., Mazurier, J., 1999. *Pseudomonas aeruginosa* binds to neoglycoconjugates bearing mucin carbohydrate determinants and predominantly to sialyl-Lewis x conjugates. *Glycobiology* **9**, 757–764.

Schneider, R.P., Chadwick, B.R., Pembrey, R., Jankowski, J., Acworth, I., 1994. Retention of the Gram-negative bacterium SW8 on surfaces under conditions relevant to the subsurface environment: effects of conditioning films and substratum nature. *FEMS Microb. Ecol.* **14**, 243–254.

Sheals, J., Sjoberg, S., Persson, P., 2002. Adsorption of glyphosate on goethite: molecular characterization of surface complexes. *Environ. Sci. Technol.* **36**, 3090–3095.

Shibukawa, M., 1995. Theoretical interpretation of the retention of system peaks in partition chromatography with a mobile phase containing electrolytes. *J. Chromatogr. A* **696**, 165–172.

Slais, K., Krejci, M., 1974. Vacant peaks in liquid chromatography. *J. Chromatogr.* **91**, 161–166.

Sposito, G., 1984. *The Surface Chemistry of Soils*. Oxford University Press, NY.

Stumm, W., Morgan, J.J., 1996. *Aquatic Chemistry: Chemical Equilibria and Rates in Natural Waters*, third ed. John Wiley, New York.

Tejedor-Tejedor, I.M., Anderson, M.A., 1990. The protonation of phosphate on the surface of goethite as studied by CIR-FTIR and electrophoretic mobility. *Langmuir* **6**, 602–611.

Tomaic, J., Zutic, V., 1988. Humic material polydispersity in adsorption at hydrous alumina/seawater interface. *J. Colloid Interface Sci.* **26**, 482–492.

Vandesteeg, H.G.M., Stuart, M.A., Dekeizer, A., Bijsterbosch, B.H., 1992. Polyelectrolyte adsorption-A subtle balance of forces. *Langmuir* **8**, 2538–2546.

Wingender, J., Neu, T.R., Flemming, H.-C., 1999. *Microbial Extracellular Polymeric Substances*. Springer-Verlag, Heidelberg, p 258.

Zeroual, W., Choisy, C., Doglia, S.M., Bobichon, H., Angiboust, J.F., Manfait, M., 1994. Monitoring of bacterial growth and structural analysis as probed by FT-IR spectroscopy. *Biochim. Biophys. Acta* **1222**, 171–178.

Zhou, Q., Maurice, P.A., Cabaniss, S.E., 2001. Size fractionation upon adsorption of fulvic acid on goethite: equilibrium and kinetic studies. *Geochim. Cosmochim. Acta* **65**, 803–812.